Large exchange bias field in Pt/Co bilayers with ultrathin native oxide

Agnieszka Klimeczek,[1] Maurizio De Santis,[1] Aurélien Masseboeuf,[2] Jan Vogel,[1] Laurent Ranno,[1] Anne Lamirand,[3] and Stefania Pizzini[1,*]

[1] *Université Grenoble Alpes, CNRS, Institut Néel, 38042 Grenoble, France*

[2] *Univ. Grenoble Alpes, CNRS, CEA, SPINTEC, 38054 Grenoble, France*

[3] *Université Lyon, Ecole Centrale de Lyon, CNRS, INSA Lyon, Université Claude Bernard Lyon 1, CPE Lyon, INL, 69130 Ecully, France*

(Dated: June 21, 2025)

We studied the magnetic properties of a Pt/Co bilayer sample with an ultrathin cobalt layer deposited as a wedge with thickness between 0.7 nm and 1.3 nm. After exposure to air, the top 0.5 nm of Co oxidises leading to a 0.9 nm-thick CoO surface layer. The residual metallic cobalt is still ferromagnetic at room temperature with a strong perpendicular magnetic anisotropy even down to ≈ 0.2-0.3 nm thickness. These properties are conserved for several months after deposition. Anomalous Hall effect measurements show the presence of an exchange bias field and a blocking temperature between 120 K and 150 K, indicating that despite being ultrathin, the CoO layer acquires antiferromagnetic order at low temperature. We attribute the large exchange bias field (up to 0.9 T at 4 K) to the ultralow thickness of the ferromagnetic Co layer. These results show that simply exposing to air an ultrathin Co layer in order to form a native CoO oxide layer, allows obtaining functional properties competing with the best reported so far for optimised Co/CoO layers and core-shell nanoparticles.

The interactions at the interface between a ferromagnetic (FM) thin film and an antiferromagnetic (AFM) layer are at the origin of many unique effects valuable for applications to spintronics devices, magnetic storage, and catalysis. The exchange bias effect[1–3], which gives rise to an increase of coercivity and a shift of the hysteresis loop due to the interface exchange-coupling between the FM and the AFM layers, has been largely studied and is currently exploited to enhance the magnetic stability of multilayered structures used in magnetic tunnel junctions. Both Co/CoO thin films[4] and Co/CoO core-shell nanoparticles[1] are model systems for the study of the effect of sample preparation, layer thickness, crystallographic order, roughness, etc, on the strength of the exchange bias field. In systems with perpendicular magnetic anisotropy (PMA) e.g. ultrathin Co deposited on a heavy metal, the Co/CoO interface is of interest as it contributes to the enhancement of the interfacial PMA[5] , which is crucial for applications to high density magnetic memories. It also contributes to the interfacial Dzyaloshinskii-Moriya interaction that allows stabilizing chiral magnetic textures such as chiral domain walls[6] and skyrmions[7]. Co/CoO thin films have also been explored as high-performance electrode materials for lithium-ion and sodium-ion batteries[8] due to their high redox activity.

We have studied the properties of a Pt/Co thin film with a gradient of Co thickness between 0.7 and 1.3 nm. After (uncontrolled) exposure to air leading to partial Co oxidation, the sample exhibits a variety of magnetic properties interesting for applications: a large PMA comparable with that of optimized Pt/Co/Pt multilayers for Co thicknesses down to 0.2-0.3 nm, a robust resistance to further oxidation and a giant exchange bias field.

A Pt(8 nm)/Co(0.7–1.3 nm) bilayer with a Ta(5 nm) underlayer was grown on a Si/SiO_2 substrate by magnetron sputtering at room temperature. The Co layer wedge with a gradient of thickness was obtained by off-axis deposition.

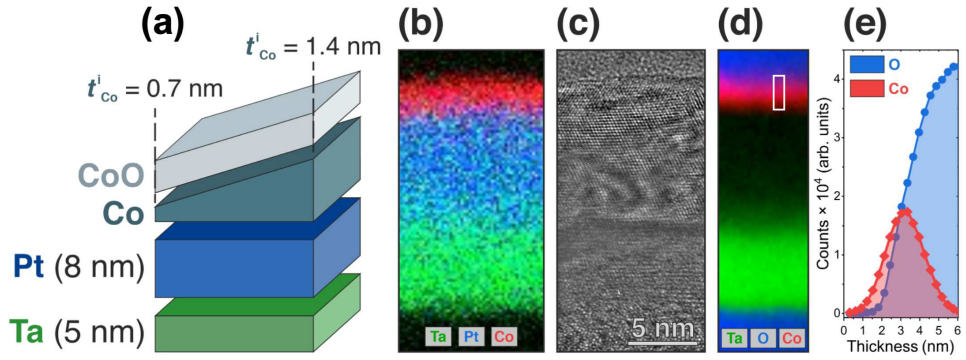

Figure 1: (a) Sketch of the Ta/Pt/Co/CoO sample with Co thickness gradient; (b-e) Transmission Electron Microscopy study of the stack in the area with ≈ 1.3 nm Co; (b) EDX image of the stack, enphasizing the different layers: Ta (green, L series), Pt (blue, L series) and Co (red, K series). (c) High Resolution Electron Microscopy image showing the crystallinity of the stack. The scale bar is the same for all images; (d) EELS map with corresponding color code for Ta (green), Oxygen (blue) and Cobalt (red). (d) profile of the EELS signal for Co and O in the area indicated by the rectangle in (d).

(Fig. 1(a)). The sample was then exposed to air leading to a partial oxidation of the cobalt layer. The thicknesses of the Ta, Pt and Co deposited layers were obtained from x-ray reflectivity measurements. Transmission electron microscopy (TEM) measurements reveal a clear Pt(111) texture which is conserved by the cobalt layer. The structure is polycrystalline with grain size of a few nanometers, well above the stack thickness. Electron Energy Loss (EELS) and Energy Dispersive X-rays (EDX) spectroscopies measurements show an interdiffusion between Pt and Co layers over ≈ 0.2 nm together with an uneven oxidation of the Co layer (Fig. 1(b-e).

The magnetic properties of the Pt/Co sample were measured with vibrating sample and superconducting quantum interference device (VSM-SQUID) magnetometry and compared with those of a reference Pt(8)/Co(0.7–1.3)/Pt(2) sample in which the Pt/Co stack under study was protected from oxidation by a 2nm-thick Pt capping layer. The hysteresis cycles versus out-of-plane (OOP) and in-plane (IP) magnetic field were measured, to access to the magnetisation per unit area $M_s t^i_{Co}$ and the in-plane saturation field as a function of the deposited cobalt thickness t^i_{Co}. The data obtained for OOP field for the uncapped Pt/Co sample are shown in Fig. 2(a). The sample exhibits an out-of-plane easy magnetisation axis, with a decreasing PMA as t^i_{Co} increases. For the largest cobalt thicknesses (around 1.3 nm) close to the reorientation transition to in-plane easy axis, the butterfly loops are characteristic of the presence of stripe domains at remanence. For each Co thickness, the magnetization per unit area of the Pt/Co sample is lower than that of the reference Pt/Co/Pt sample (Fig. 2(b)): This is not surprising as part of the Co layer is expected to oxidize when exposed to atmospheric conditions. Assuming that the saturation magnetisation does not change with t^i_{Co}[9], the thickness of the unoxidised Co layer, t_{Co}, can be extracted from the ratio of $M_s t^i_{Co}$ in the two sets of measurements (Fig. 2(c)). We therefore find that, all along the wedge, the top ≈0.5 nm of cobalt oxidises and t_{Co} is reduced to only ≈ 0.2-0.3 nm i.e. 1-2 monolayers (MLs) on the thinnest part of the wedge sample. Even within the error bars associated to the measurement of Co thicknesses, the saturation magnetisation M_S for both the Pt/Co and the Pt/Co/Pt layers is larger than that of Co bulk. This is attributed to the moment acquired by Pt when in

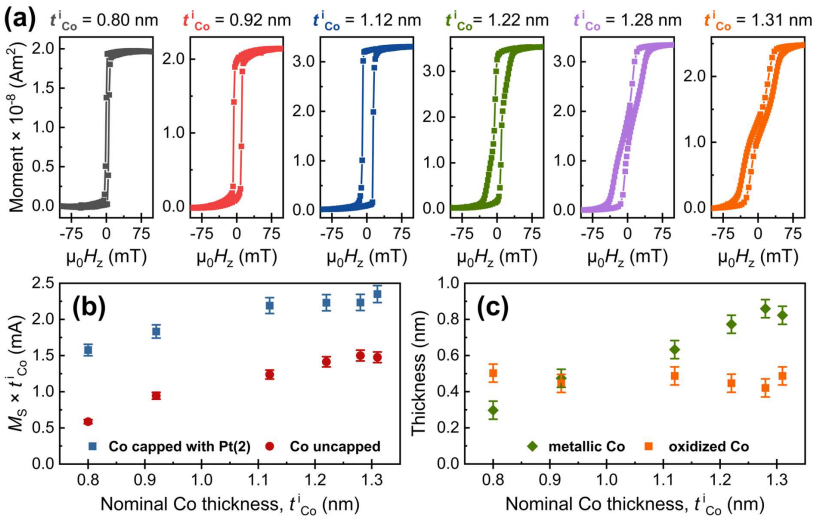

Figure 2: (a) Hysteresis cycles measured by VSM-SQUID with out-of-plane magnetic field for uncapped Pt/Co sample for increasing Co thickness; (b) magnetisation per unit area for the Pt/Co and the reference Ta/Pt/Co/Pt samples as a function of deposited Co thickness; (c) thickness of unoxidised Co and oxidised Co layers in the uncapped Pt/Co sample versus deposited (nominal) Co thickness.

contact with Co (see Ref.[10]) and to the enhanced orbital moment of Co at the Co/CoO interface[11,12].

The in-plane saturation field is maximum (≈1.5 T) for the sample position with thinnest Co. The associated effective magnetic anisotropy (≈ 1MJ/m^3) is comparable to that reported for optimised Pt/Co(0.3 nm)/Pt multilayers in Ref.[9]. This infers that the Co/oxide interface formed by natural oxidation gives a contribution to the PMA of the same order of magnitude as that of the Pt/Co interface.

To characterize the nature of the native Co oxide, we carried out Co 2p x-ray photoelectron spectroscopy (XPS) measurements for three Co thicknesses (t^i_{Co} = 0.85, 1.05 and 1.3 nm) and with two (or three) collection angles θ of the photoemitted electrons. Fig. 3(a,b) shows the spectra measured for 0.85 nm and 1.3 nm Co thicknesses with θ=0° and 60°. The spectra were deconvoluted considering main and satellite peaks of metallic Co and Co oxide, a strong Shirley plus linear background as well as overlapping MLN Auger peaks, as the data were acquired using Al Kα_1 radiation (hν=1486.6 eV) source. The binding energy scale was calibrated using the Pt $4f_{7/2}$ core level (71 eV), leading to O 1s peak at 529.4 eV. No charging effect was observed.

For both 0.85 nm and 1.3 nm Co layers, the spectra present two main peaks, corresponding to CoO $2p_{1/2}$ and CoO $2p_{3/2}$ core levels (lying at 797 eV and 781 eV ± 0.4eV), respectively, and two satellite peaks (lying at 802 eV and 785.5 eV ± 0.4 eV) that arise from the charge transfer between O 2p and Co 3d electronic levels[13]. This charge transfer allows the coexistence of two transitions: $2p^6d^7 \rightarrow 2p^5 3d^7 + e^-$ (satellite peaks) and $2p^6d^8L \rightarrow 2p^5 3d^8 L + e^-$ (main peaks) where L is a hole in the oxygen ligand[14].

The weak contribution from metallic Co appears as a shoulder of the two CoO peaks, with binding energies of

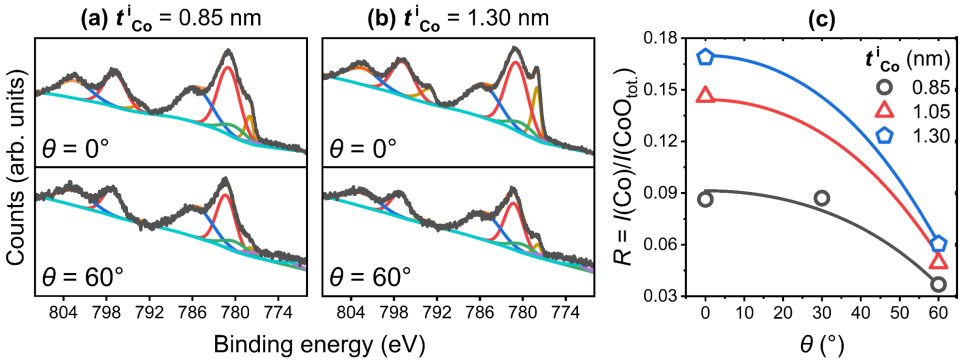

Figure 3: (a-b) Co 2p XPS spectra for the uncapped Pt/Co sample with t^i_{Co} = 0.85 and 1.3 nm: raw data (black), Shirley plus linear background (light blue), deconvolution into metallic Co peaks (brown), CoO peaks (red and blue) and Auger peak (green); (c) ratio of the intergrated intensities of the Co and CoO peaks for three Co thicknesses as a function of the collection angle of photoemitted electrons, for three t^i_{Co} thicknesses

793.3 eV and 778.1 eV[13,15]. As expected, the intensity of the metallic peaks is larger for the thicker Co layer. On the other hand, the reduction of the metallic peaks in the spectra taken with collection angle 60° (grazing) indicates that the CoO layer is formed at the sample surface. The ratio between the intensity of the metallic peak and the total intensity of the CoO peaks is shown in Fig. 3(c) as a function of collection angle. The largest contribution of the metallic Co is around 17% and is found for the 1.3 nm Co layer with collection angle 0°. Taking into account an attenuation length of ≈0.8nm for the emitted photoelectrons[16], the results of the quantitative analysis of the spectra[17] are consistent with a CoO thickness of ≈ 0.9 nm. This value is in agreement with the results of the VSM-SQUID data since when oxidised to CoO, the top 0.5 nm of Co acquire a thickness of ≈0.9 nm[18].

These results can be discussed in the framework of the detailed work carried out by Smardz et al.[19] on the oxidation kinetics of thin and ultrathin Co layers deposited on a Si/SiO_2 substrate. The authors found that Co layers thicker than 5 nm oxidised quasi instantaneously with 2.5 nm of Co metal transformed into oxide. For Co layers thinner than 5 nm the time constant for oxidation increased considerably and followed an approximately linear dependence with decreasing film thickness. Layers thinner than 2.5 nm kept ferromagnetic character for the time of the study (more than 150 days) which allowed them to state that Co is ferromagnetic at room temperature (RT) down to the ML regime. The authors attributed the slower oxidation of Co to a better growth near the substrate which leaves less paths for oxygen transport.

Similarly to the cited work, we find that the oxidation process in our samples is very slow since, one year after the deposition, the Co layer all along the wedge is still ferromagnetic at RT. A slight increase of anisotropy, suggested by the increased squareness of the hysteresis loops for the thickest Co, suggests that the Co oxide thickness has increased with time; nevertheless the thinnest deposited Co layer is still ferromagnetic, although after oxidation its metallic part is reduced to a thickness of less than 0.3 nm. Contrary to Ref.[19], when deposited on Pt with a strong (111) texture the ultrathin cobalt layer conserves a strong PMA at RT and, as we will show below, also a strong exchange bias at low temperature.

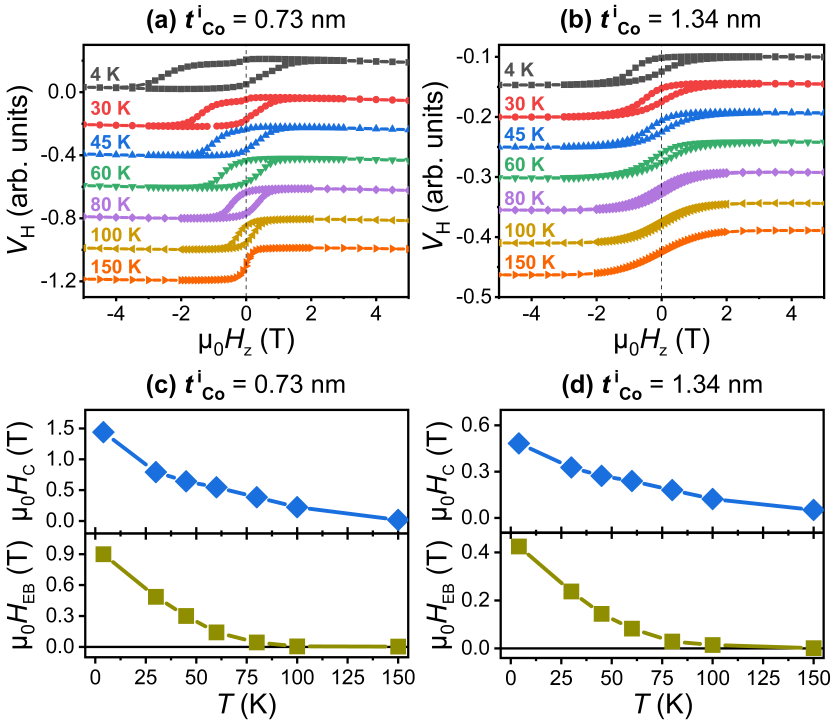

Figure 4: Anomalous Hall effect measurements: (a-b) hysteresis loops measured with a B_z magnetic field after field-cooling with +5 T for the uncapped Pt/Co sample with t^i_{Co}=0.73 nm (a) and 1.34 nm (b); (c-d) coercive field and exchange bias field as a function of temperature for the two deposited Co thicknesses.

Bulk CoO is antiferromagnetic with a Néel temperature of 293 K[20]. In order to prove that the ultrathin CoO oxide obtained by natural oxidation of the Co layer can be antiferromagnetically ordered, we patterned the sample into Hall crosses and we carried out anomalous Hall effect measurements. After field-cooling the samples under an out-of-plane magnetic field of +5 T, hysteresis cycles were measured between 4 K and 150 K. The coercivity strongly increases and a large shift of the hysteresis loops is observed.

Fig. 4 shows the measurements carried out for a thin (t^i_{Co}= 0.73 nm) and a thick (t^i_{Co}=1.34 nm) Co layer, together with the variation of the coercivity and the exchange bias field versus temperature. At 4 K, a very large exchange bias field $\mu_0 H_{EB}$=0.9 T is observed for the thin Co. This field is reduced to 0.42 T for the thick Co, in agreement with the fact that $H_{EB} \propto 1/t_{FM}$ (see Ref.[2]). The extrapolation of the curves indicates that the blocking temperature is around 120 K for the thin Co and increases to 150 K for the thick Co. These results indicate that the 0.9 nm-thick CoO layer exceeds the critical oxide thickness d_{crit} necessary for a field offset to appear. From Mauri et al.[21] $d_{crit} = J_i/K_{CoO}$ where J_i=$\mu_0 H_{EB} t_{Co} M_s$ is the interface exchange energy, $M_s t_{Co}$ is the saturation magnetisation per unit surface and K_{CoO} is the volume anisotropy energy of the AF layer. For the thin Co layer $J_i \approx 0.54$ mJ/m^2 and from $d_{crit} \leq 0.9$

nm we obtain that $K_{CoO} \geq 0.6$ MJ/m^3 at 4 K. This large value of the CoO volume anisotropy energy which is at the origin of the exchange bias, is of the same order of magnitude as that obtained by Smardz et al.[19].

Note that the large EB field measured at 4 K exceeds the best values that we found in the literature for both core-shell Co/CoO nanoparticles (NPs) and Co/CoO films. Mohopatra et al.[22] reported $\mu_0 H_{EB}$=0.36 T at 5 K for NPs with 12 nm average diameter with an amorphous CoO shell; Gandha et al.[23] found $\mu_0 H_{EB}$=0.24 T at 10 K for 14 nm diameter core-shell nanowires. Concerning films, Sun et al.[24] reported the largest bias field of 0.7 T at 2 K for Co/CoO bilayers deposited on a flexible substrate. Much lower values were otherwise measured (see Sun et al.[24] and references therein). In all these works the Co magnetisation lies in the plane of the layers. Only a few works[25,26] have reported the presence of exchange bias in Co/CoO films with perpendicular easy-axis. Matt et al.[26] compared the exchange bias field at 10 K obtained for a $(Pt/Co)_5$/Co/CoO multilayer with field cooling parallel and perpendicular to the surface plane; the much larger EB field found with the field applied in-plane (89 mT) with respect to OOP (43 mT) was related to the larger projection of the CoO easy magnetization direction along the cooling field. We attribute the large EB field measured in our Pt/Co/CoO layer with ultrathin (0.2-0.3 nm) metallic Co, to the much lower thickness of the FM layer, compared to the works reported above. Note also that the estimated interface exchange energy J_i is comparable to the values reported in the literature for samples in which the CoO growth has been optimised[22,24,27] and twice as large as that reported by Matt et al.[26] for a sample with PMA cooled with the OOP field.

The blocking temperatures T_B measured in this work (up to 150 K for the Pt/Co sample with the thickest Co film) are lower than the Néel temperature T_N of bulk CoO. This is a general feature found in the literature that is attributed to finite size effect of T_N i.e. the decrease of the Néel temperature as the AF thickness decreases[24,28,29]. A fast decrease of both T_B and H_{EB} for decreasing CoO thickness was reported for instance for a FeNi/CoO system for $t_{CoO} \leq 10$ nm[29]. Also, the Néel temperature of epitaxial NiO(100)/MgO(100) was shown to strongly decrease for thicknesses below 20 MLs[28]. Sun et al.[24] report a blocking temperature of 195 K for a CoO thickness of around 5 nm. In this respect, it is remarkable that relatively high T_B are found in our samples where the CoO thickness is around 1 nm. The microscopic understanding of this effect is under investigation.

In conclusion we have shown that upon exposure to air the Pt/Co(0.7-1.3 nm) stack partially oxidises with the formation of an ultrathin CoO layer ($\approx$ 0.9 nm), as shown by XPS measurements. The sample remains ferromagnetic with large PMA for several months, even for the thinnest layer consisting of only 0.2-0.3 nm of metallic Co. Anomalous Hall effect measurements show that the ultrathin CoO layer acquires antiferromagnetic order at low temperature, as indicated by the large exchange bias field - 0.9 T for (0.2-0.3 nm) thin Co to 0.42 T for (0.8-0.9 nm) thick Co - observed after field cooling. These results show that simply exposing to atmospheric conditions our ultrathin cobalt in order to form a native CoO oxide, allows obtaining functional properties competing with the best reported so far for optimised samples[4,30].

I. ACKNOWLEDGMENTS

This work was supported by France 2030 government plan managed by the Agence Nationale de la Recherche (project PEPR SPIN CHIREX ANR-22-EXSP-0002). We acknowledge the METSA network for supporting the TEM experiments conducted at the CEA Grenoble nano-characterization platform. B. Fernandez, T. Crozes, Ph. David,

D. Barral, E. Mossang, P. Lachkar and E. Wagner are acknowledged for their technical help at Institut Néel.

* Electronic address: stefania.pizzini@neel.cnrs.fr

[1] W. H. Meiklejohn and C. P. Bean, Phys. Rev. **102**, 1413 (1956).
[2] J. Nogués and I. K. Schuller, Journal of Magnetism and Magnetic Materials **192**, 203 (1999).
[3] J. Nogués, J. Sort, V. Langlais, V. Skumryev, S. Suriñach, J. Muñoz, and M. Baró, Physics Reports **422**, 65 (2005).
[4] T. Blachowicz and A. Ehrmann, Coatings **11**, 122 (2021).
[5] B. Dieny and M. Chshiev, Rev. Mod. Phys. **89**, 025008 (2017).
[6] A. Thiaville, S. Rohart, E. Jué, V. Cros, and A. Fert, Europhysics Letters **100**, 57002 (2012).
[7] A. Fert, N. Reyren, and V. Cros, Nat. Rev. Mater. **2**, 17931 (2017).
[8] M. Sun, H. Zhang, Y.-F. Wang, W.-L. Liu, M.-M. Ren, F.-G. Kong, S.-J. Wang, X.-Q. Wang, X.-L. Duan, and S.-Z. Ge, Journal of Alloys and Compounds **771**, 290 (2019), ISSN 0925-8388.
[9] C.-J. Lin, G. Gorman, C. Lee, R. Farrow, E. Marinero, H. Do, H. Notarys, and C. Chien, Journal of Magnetism and Magnetic Materials **93**, 194 (1991), ISSN 0304-8853.
[10] W. Grange, M. Maret, J.-P. Kappler, J. Vogel, A. Fontaine, F. Petroff, G. Krill, A. Rogalev, J. Goulon, M. Finazzi, et al., Phys. Rev. B **58**, 6298 (1998).
[11] T. Ueno, J. Sinha, N. Inami, Y. Takeichi, S. Mitani, K. Ono, and M. Hayashi, Scientific Reports **50**, 14858 (2015).
[12] Z. Zhang, X. Lu, Z. Li, Z. Li, Y. Yan, Y. Chen, J. Du, F. Zhu, J. Cao, Y. Wang, et al., AIP Advances **14**, 025049 (2024).
[13] M. C. Biesinger, B. P. Payne, A. P. Grosvenor, L. W. Lau, A. R. Gerson, and R. S. Smart, Applied Surface Science **257**, 2717 (2011).
[14] G. A. Carson, M. H. Nassir, and M. A. Langell, Journal of Vacuum Science Technology A **14**, 1637 (1996).
[15] M. Sicot, S. Andrieu, F. Bertran, and F. Fortuna, Phys. Rev. B **72**, 144414 (2005).
[16] A. Jablonski and C. Powell, Journal of Electron Spectroscopy and Related Phenomena **199**, 27 (2015).
[17] A. Jablonski and C. J. Powell, Journal of Physical and Chemical Reference Data **49**, 033102 (2020).
[18] A. Jain, S. P. Ong, G. Hautier, W. Chen, W. D. Richards, S. Dacek, S. Cholia, D. Gunter, D. Skinner, G. Ceder, et al., APL Materials **1**, 011002 (2013).
[19] L. Smardz, U. Köbler, and W. Zinn, Journal of Applied Physics **71**, 5199 (1992).
[20] Néel, M. L., Ann. Phys. **12**, 137 (1948).
[21] D. Mauri, E. Kay, D. Scholl, and J. K. Howard, Journal of Applied Physics **62**, 2929 (1987).
[22] J. Mohapatra, M. Xing, R. Wu, J. Yang, and J. P. Liu, Scripta Materialia **230**, 115400 (2023).
[23] K. Gandha, R. P. Chaudhary, J. Mohapatra, A. R. Koymen, and J. P. Liu, Physics Letters A **381**, 2092 (2017), ISSN 0375-9601.
[24] Y. Sun, W. Tang, S. Chen, L. Liu, H. Liu, J.-Y. Ge, X. Zhang, W.-C. Jiang, H. Liang, and Y.-J. Zeng, Advanced Physics Research **2**, 2200066 (2023).
[25] E. Shipton, K. Chan, T. Hauet, O. Hellwig, and E. E. Fullerton, Applied Physics Letters **95**, 132509 (2009).
[26] S. Maat, K. Takano, S. S. P. Parkin, and E. E. Fullerton, Phys. Rev. Lett. **87**, 087202 (2001).
[27] M. Gruyters and D. Riegel, Journal of Applied Physics **88**, 6610 (2000).
[28] D. Alders, L. H. Tjeng, F. C. Voogt, T. Hibma, G. A. Sawatzky, C. T. Chen, J. Vogel, M. Sacchi, and S. Iacobucci, Phys. Rev. B **57**, 11623 (1998).
[29] T. Ambrose and C. L. Chien, Journal of Applied Physics **83**, 6822 (1998).
[30] A. Sharma, J. Tripathi, S. Tripathi, Y. Kumar, K. Ugochukwu, D. Kumar, M. Gupta, and R. Chaudhary, Journal of

Magnetism and Magnetic Materials **510**, 166599 (2020).